Journal of King Saud University – Computer and Information Sciences (2013) **25**, 117–126

King Saud University

Journal of King Saud University – Computer and Information Sciences

www.ksu.edu.sa
www.sciencedirect.com

ORIGINAL ARTICLE

A genetic algorithm for the level control of nulls and side lobes in linear antenna arrays

Bipul Goswami, Durbadal Mandal *

Department of Electronics and Communication Engineering, National Institute of Technology Durgapur, West Bengal 713 209, India

Received 3 January 2012; revised 4 June 2012; accepted 26 June 2012
Available online 4 July 2012

KEYWORDS

Side lobe level;
Deeper nulls;
Real coded genetic algorithm;
Linear antenna array;
First null beam width

Abstract The design problem of imposing deeper nulls in the interference direction of uniform linear antenna arrays under the constraints of a reduced side lobe level (SLL) and a fixed first null beam width (FNBW) is modeled as a simple optimization problem. The real-coded genetic algorithm (RGA) is used to determine an optimal set of current excitation weights of the antenna elements and the optimum inter-element spacing that satisfies the design goal. Three design examples are presented to illustrate the use of the RGA, and the optimization goal in each example is easily achieved. The numerical results demonstrate the effectiveness of the proposed method.
© 2013 Production and hosting by Elsevier B.V. on behalf of King Saud University.

1. Introduction

An antenna array is composed of an assembly of radiating elements in an electrical or geometrical configuration. In most cases, the elements are identical. The total field of the antenna array is found by vector addition of the fields radiated by each individual element. Five controls in an antenna array can be used to shape the pattern properly: the geometrical configuration (linear, circular, rectangular, spherical) of the overall array, the spacing between the elements, the excitation amplitude of the individual elements, the excitation phase of the individual elements, and the relative pattern of the individual elements (Ballanis, 1997; Elliott, 2003). Many communication applications require a highly directional antenna. Array antennas have higher gain and directivity than an individual radiating element. A linear array consists of elements placed in a straight line with a uniform spacing between the elements (Haupt and Werner, 2007). The goal of antenna array geometry synthesis is to determine the physical layout of the array that produces a radiation pattern that is closest to the desired pattern.

The increasing amount of electromagnetic pollution has prompted the study of array pattern nulling techniques. These techniques are important in radar, sonar and communication systems to minimize degradation of the signal to noise ratio due to undesired interference (Haupt and Werner, 2007). Much current research on antenna arrays (Haupt, 1997; Steyskal et al., 1986; Yang et al., 2004; Mandal et al., 2010; Guney and Akdagli, 2001) is focused on using robust and easily adapted optimization techniques to improve the nulling performance. Classical gradient-based optimization methods are not suitable for improving the nulling performance of linear antenna arrays for several reasons, including the following:

* Corresponding author. Tel.: +91 9474119721.
E-mail address: durbadal.bittu@gmail.com (D. Mandal).
Peer review under responsibility of King Saud University.

Production and hosting by Elsevier

1319-1578 © 2013 Production and hosting by Elsevier B.V. on behalf of King Saud University.
http://dx.doi.org/10.1016/j.jksuci.2012.06.001

(i) the methods are highly sensitive to the starting points when the number of variables, and hence the size of the solution space, increases, (ii) they frequently converge to local optimum solutions, diverge or arrive at the same suboptimal solution, (iii) they require a continuous and differentiable objective function (gradient search methods), (iv) they require piecewise linear cost approximation (linear programming), and (v) they have problems with convergence and algorithm complexity (non-linear programming). Thus, evolutionary optimization methods have been employed for the optimal design of deeper nulls. Different evolutionary optimization algorithms, such as fuzzy logic (Mukherjee and Kar, 2012; Anooj, 2012; De and Sil, 2012), the bees algorithm (Fahmy, 2012), the genetic algorithm (GA) (Haupt and Werner, 2007), and particle swarm optimization (PSO) (Mandal et al., 2012), have been widely used in the development of design methods that are capable of satisfying constraints that would otherwise be unattainable. Of these algorithms, GA is a promising global optimization method for the design of antenna arrays.

Several methods for the synthesis of array antenna patterns with prescribed nulls are reviewed below. A method for null control and the effects on radiation patterns is discussed in Steyskal et al. (1986). An approach of null control using PSO, where single or multiple wide nulls are generated by optimum perturbations of the elements' current amplitude weights to create symmetric nulls about the main beam, is discussed in Mandal et al. (2010). An approach for the pattern synthesis of linear antenna arrays with broad nulls is described in Guney and Akdagli (2001). In Yang et al. (2002), a differential evolution algorithm is used to optimize the static-mode coefficients and the durations of the time pulses, leading to a significant reduction of the sideband level. A binary coded genetic algorithm is used in Haupt (1995, 1975) and Yan and Lu (1997) to reduce the sidelobe level of a linear array by excitation coefficient tapering. The spacing is assumed to be equal to half of the wavelength throughout the array aperture. The study shows good sidelobe performance (approximately -33 dB) for a 30 element array. The radiation pattern of linear arrays with large numbers of elements (20–100) is improved using a GA in Ares-Pena et al. (1999). The sidelobes for 20 and 100 element arrays are reduced to -20 dB and -30 dB, respectively. A decimal GA technique to taper the amplitude of the array excitation to achieve reduced side lobe and null steering in single or multiple beam antenna arrays is proposed in Abdolee et al. (2007). In Son and Park (2007), a low-profile phased array antenna with a low sidelobe was designed and fabricated using a GA. The sidelobe level was suppressed by only 6.5 dB after optimization. An approach for sidelobe reduction in a linear antenna array using a GA is proposed in Recioui et al. (2008), Das et al. (2010). In Das et al. (2010), the sidelobes for symmetric linear antenna arrays are reduced without significantly sacrificing the first null beamwidth, and non-uniform excitations and optimal uniform spacing are proposed generate the desired result. Optimal values are found using the real-coded genetic algorithm (RGA). An approach to determine an optimum set of weights for antenna elements to reduce the maximum side lobe level (SLL) in a concentric circular antenna array (CCAA) with the constraint of a fixed beamwidth is proposed in Mandal et al. (2009), Mondal et al. (2010). In (Cafsi et al. (2011), a method of adaptive beamforming is described for a phased antenna array using a GA. The algorithm can determine the values of phase excitation for each antenna to steer the main beam in specific directions.

The goal of this paper is to introduce deeper null/nulls in the interference directions and to suppress the relative SLLs with respect to the main beam with the constraint of a fixed first null beam width (FNBW) for a symmetric linear antenna array of isotropic elements. This is done by designing the relative spacing between the elements with a non-uniform excitation over the array aperture. An evolutionary technique, the RGA (Haupt and Werner, 2007; Haupt, 1995; Holland, 1975), is used to obtain the desired pattern of the array. Several aspects of the RGA are different from other search techniques. First, the algorithm is a multi-path technique that searches many peaks in parallel and hence decreases the possibility of local minimum trapping. Secondly, the RGA only needs to evaluate the objective function (fitness) to guide its search. Hence, there is no need to compute derivatives or other auxiliary functions, so the RGA can also minimize the non-derivable objective function. Finally, the RGA explores the search space where the probability of finding improved performance is high.

A broadside uniform linear array with uniform spacing is considered. The array is symmetric with respect to the origin with equal spacing between any two consecutive elements. The phase difference between any two elements is fixed at zero. The RGA adjusts the excitation coefficients and location of the elements from the array center to impose deeper nulls in the interference directions. A cost function is defined that keeps the nulls and side lobes at lower levels.

The remainder of the paper is arranged as follows. In Section 2, the general design equations for a non-uniformly excited and unequally spaced linear antenna array are stated. A brief introduction to the Genetic Algorithm is presented in Section 3, and the numerical simulation results are presented in Section 4. The paper concludes with a summary of the work in Section 5.

2. Design equation

A broadside linear antenna array (Ballanis, 1997; Elliott, 2003) of $2M$ isotropic radiators, as shown in Fig. 1, is considered. Each element is excited with a non-uniform current. The array elements are assumed to be uncoupled and equally spaced along the z-axis, and the center of the array is located at the origin. The array is symmetric in both geometry and excitation with respect to the center.

The radiation characteristics of antennas are most important in the far field (*Fraunhofer*) region. An array consisting of identical and identically oriented elements has a far field radiation pattern that can be expressed as the product of the element pattern and a factor that is widely referred to as the array factor. Each array has its own array factor. The array factor, in general, is a function of the number of elements, their geometrical arrangement, their relative magnitudes, their relative phases, and their relative spacings. Because the array factor does not depend on the directional characteristics of the radiating elements, it can be formulated by replacing the actual elements with isotropic (point) sources. For the array in Fig. 1, the array factor, $AF(I, \varphi, d)$ Ballanis, 1997; Elliott, 2003 in the azimuth plane (x–y plane) with symmetric amplitude distributions (Ballanis, 1997) may be written as (1):

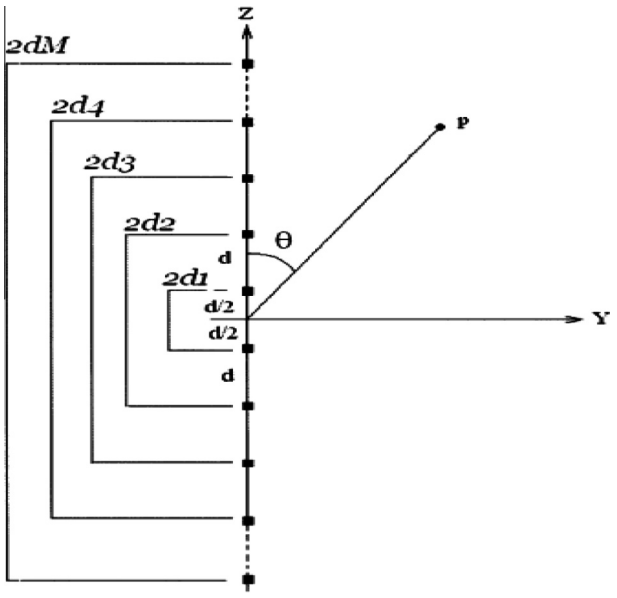

Figure 1 Geometry of a $2M$ element symmetric linear antenna array along the z axis.

$$AF(I,\varphi,d) = 2\sum_{n=1}^{M} I_n \cos\left[\left(\frac{2n-1}{2}\right)kd\cos(\theta)+\varphi_n\right] \quad (1)$$

where θ denotes the zenith angle measured from the broadside direction of the array, I_n and φ_n are the current excitation amplitude and the excitation phase of the nth array element, respectively, d is the spacing between two consecutive elements and $k = 2\pi/\lambda$ are the wave numbers, where λ is the signal wave-length. In this paper, φ_n is fixed at zero. The array elements are numbered from 1 to M from the origin in a symmetric array, where the total number of elements is $2M$.

After defining the far-field radiation pattern, the next step in the design process is to formulate the objective function that is to be minimized. The objective function is defined using the array factor in such a way that the objective of the optimization is satisfied. For the optimization problem of the null placement in the far field pattern of the array, the array factor value at the particular null position must be less than the reference pattern. Similarly, for the side lobe reduction problem, the array factor values at the side lobe peaks must be less than the reference pattern. To satisfy these objectives, the array factor is included in the cost function expression. The objective function "cost function" (CF) to be minimized with the RGA to introduce the deeper null and reduce the relative SLL is given in (2):

$$CF = C_1 \times \frac{\left|\prod_{i=1}^{m} AF(null_i)\right|}{|AF_{\max}|} + C_2 \times \sum_{k=1}^{K} H(k)\times(Q_k-\delta) + C_3 \times \left(\mathrm{FNBW}_{computed} - \mathrm{FNBW}(I_n=1)\right) \quad (2)$$

where m is the maximum number of positions where the null can be imposed. In this paper, the value of 'm' is considered to be one and two. $AF(null_i)$ is the value of the array factor at the particular null position, and $AF_{\max}$ is the maximum value of the array factor. The second term in (2) is summed to reduce the SLL to a desired level. K denotes the number of side lobes in the original pattern, Q_k is the side lobe level in dB generated by the individual population at some peak point θ_k, and δ is the desired value of the side lobe level in dB. $H(k)$ is defined as (3):

$$H(k) = \begin{cases} 1, & (Q_k-\delta) > 0 \\ 0, & (Q_k-\delta) \leqslant 0 \end{cases} \quad (3)$$

The side lobes whose peaks exceed the threshold δ must be suppressed, so $H(k)$ is adopted in the "cost function" expression. FNBW denotes the first null beamwidth, which is the angular width between the first nulls on either side of the main beam. The third term in (2) is introduced to keep FNBW of the optimized pattern the same as in the initial pattern (the pattern for $I_n = 1$ and $d = \lambda/2$). In (2), the two beamwidths $\mathrm{FNBW}_{computed}$ and $\mathrm{FNBW}(I_n = 1)$ refer to the computed first null beamwidth in radian for the non-uniform excitation for the optimal spacing case and for the uniform excitation $(I_n = 1)$ with uniform inter-element spacing $(d = \lambda/2)$ case, respectively. The actual value of FNBW for a uniform linear array can be calculated by (4):

$$\theta_n = \frac{2\lambda}{Nd} \quad (4)$$

where $N\ (= 2M)$ is the total number of elements in the array. C_1, C_2, and C_3 are weighting coefficients to control the relative importance of each term of (2). Because the primary aim is to achieve a deeper null, the value of C_1 is higher than the values of C_2 and C_3. In the first term of (2), both the numerator and denominator are absolute values. A smaller value of the cost function means that the array factor values at predefined positions are lower. Consequently, RGA controls the amplitude excitations and the inter-element spacing to minimize the cost function.

3. Evolutionary optimization technique: genetic algorithm

Genetic algorithms are a family of computational models inspired by evolution (Haupt and Werner, 2007; Haupt, 1995; Holland, 1975). GAs can be used to find approximate solutions to search problems through the application of the principles of evolutionary biology. GA uses biologically inspired techniques, such as genetic inheritance, natural selection, mutation, and sexual reproduction (recombination or crossover). The GA was first introduced in 1975 by Prof. Holland (1975). Real-coded GA (RGA) uses floating-point number representations for the real variables and thus is free of binary encoding and decoding. Hence, it is faster than binary GA. The algorithm performs the following steps:

(1) Randomly or heuristically generates an initial population within the variable constraint range.
(2) Computes and saves the fitness for each individual in the current population.
(3) Defines the selection probability for each individual so that it is proportional to its fitness.
(4) Generates the next population by probabilistically selecting the individuals from the previous current population to produce offspring via genetic operators.
(5) Repeats step 2 until a satisfactory solution is obtained.

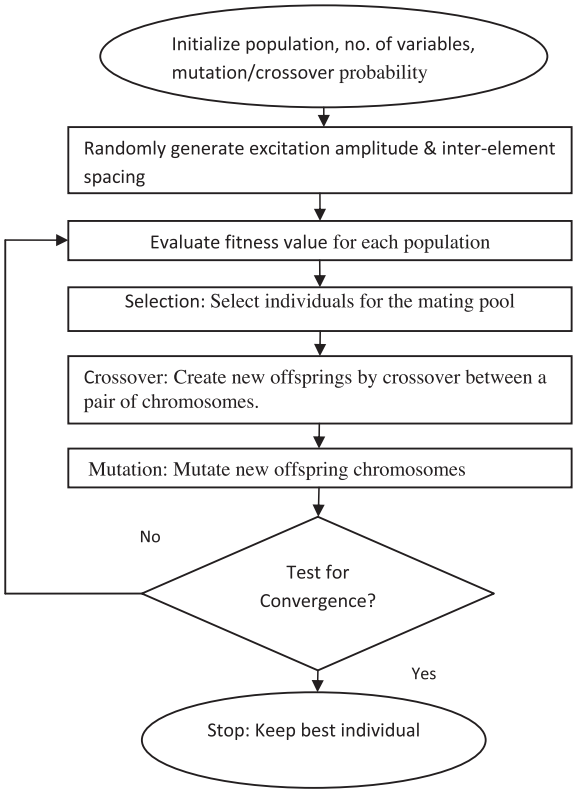

Figure 2 The GA flow for determining the optimized excitation amplitude and optimum location of array elements.

GA consists of a data structure of individuals called the population. Individuals are also called chromosomes. Each chromosome is evaluated by a function known as a fitness function or a cost function, which is usually the fitness function or the objective function of the corresponding optimization problem.

The working principle of a GA is explained briefly in Fig. 2 based on the problem addressed in this paper.

The important parameters of the GA are as follows:

- **Selection** – this is based on the fitness criterion to choose which chromosome from a population will go onto reproduce.
- **Reproduction** – the propagation of individuals from one generation to the next.
- **Crossover** – this operator exchanges genetic material, which are the features of the optimization problem. Single point crossover is used here.
- **Mutation** – the modification of chromosomes in single individuals. Mutation does not permit the algorithm to get stuck at a local minimum.

Stopping criteria – The iteration stops when the maximum number of cycles is reached. The grand minimum *CF* and its corresponding chromosome string or the desired solution are finally obtained.

The desired pattern is generated by jointly optimizing the amplitude distributions and the inter-element spacing with the fixed first null beam width. In this paper, both the amplitude and the inter-element spacing distributions are assumed to be symmetric with respect to the center of the array. The chromosomes correspond to the current excitation weights and the inter-element spacing of the antenna elements. Because of symmetry, each chromosome consists of $M + 1$ number of genes, where M is the number of antenna elements on either side of the array center. Here, the 1st to M^{th} genes represent the current excitation weights of the antenna elements, and the $(M+1)^{\text{th}}$ gene represents the inter-element spacing. For example, chromosome one $\overline{W}_1$ can be represented by (5):

$$\overline{W}_1 = [W_{11}, W_{12}, \ldots W_{1M}, W_{1(M+1)}] \tag{5}$$

where $W_{11}, W_{12}, \ldots W_{1M}$ are the antenna element weights or genes, and $W_{1(M+1)}$ is the inter-element spacing. Each of these current excitation weights and the inter-element spacing has upper and lower limits. The random set of chromosomes can easily be constructed using the following relation represented by (6):

$$\overline{W}_n = (u_1 - u_2) \times \bar{r} + u_2, u_2 < \overline{W}_n \leqslant u_1 \tag{6}$$

where u_1 and u_2 are the maximum and minimum limit values of the weights, respectively, and $\bar{r}$ is a real random vector between zero and one. All of the current excitation weights are restricted to lie between 0 and 1, and the inter-element spacing is restricted to lie between $\lambda/2$ and λ.

4. Numerical simulation results

Linear antenna arrays composed of 12, 16, and 20 isotropic radiating elements, with an inter-element spacing of λ/2, are considered for reference. RGA is applied to obtain deeper nulls and to reduce the SLLs. RGA was executed with 500 iterations, and the population size was fixed at 120. For the RGA, the mutation probability was set to 0.05, and uniform crossover was used. The RGA algorithm is initialized using random values of the excitation ($0 < I_n < 1$) and the spacing between the elements ($\lambda/2 \leqslant d < \lambda$). The nulling performances are improved for predefined nulls of the radiation pattern. Similarly, nulls are imposed at predefined peak positions. The program was written in Matlab and run in MATLAB version 7.8.0(R2009a) on a 3.00 GHz core (TM) 2 duo processor with 2 GB RAM.

The initial values of the maximum side lobe level (SLL) and the FNBW for a uniform amplitude ($I_n = 1$) and uniform spacing ($\lambda/2$ between adjacent elements) for all of the array structures (linear arrays with 12, 16 and 20 elements) are given in Table 1.

Figs. 3–5 show the generation of deeper nulls over the 3rd null. For the 12, 16, and 20-element arrays, the nulls have improved up to −79.54 dB, −80 dB, and −98.51 dB from the initial values of −51.90 dB, −50.60 dB, and −77.20 dB, respectively. Table 2 shows the resulting amplitude excitation

Table 1 SLL and FNBW for uniform excitation ($I_n = 1$) of linear array sets with an inter-element spacing of $\lambda/2$.

Set no.	Total number of elements ($2M$)	SLL (dB)	FNBW (degrees)
I	12	−13.06	19.10
II	16	−13.14	14.40
III	20	−13.19	11.52

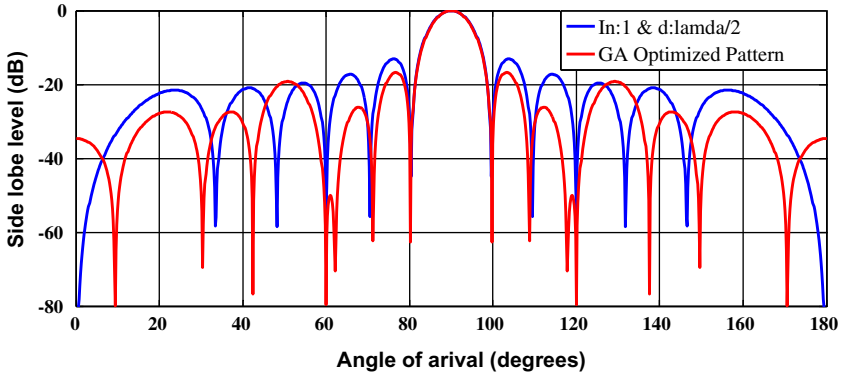

Figure 3 Best array pattern found by RGA for the 12-element array case with an improved null at the 3rd null; i.e., $\theta = 60°$ and $\theta = 120°$.

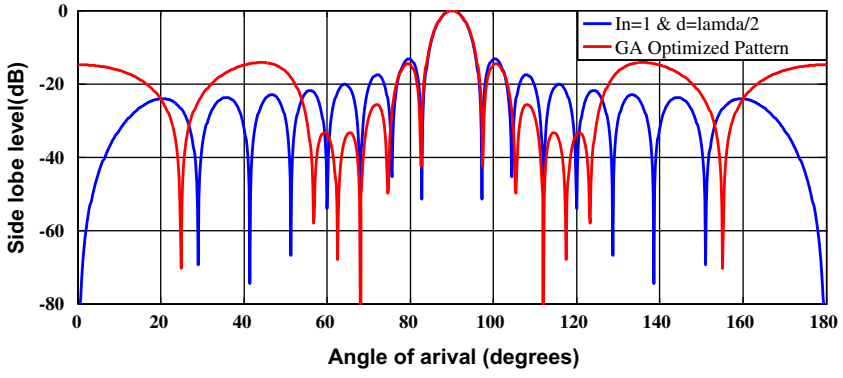

Figure 4 Best array pattern found by RGA for the 16-element array case with an improved null at the 3rd null; i.e., $\theta = 68°$ and $\theta = 112°$.

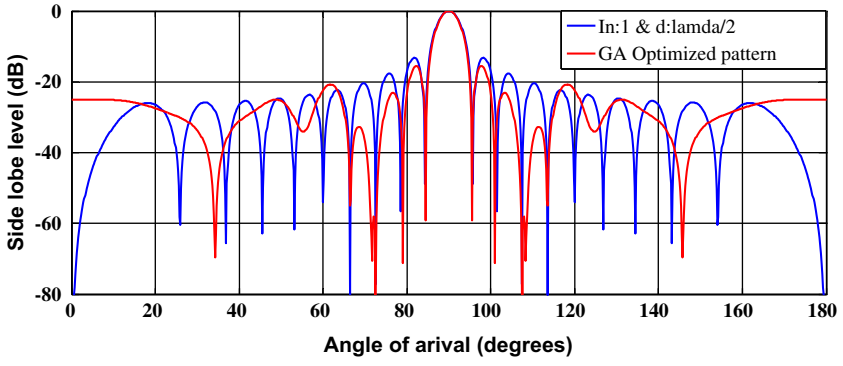

Figure 5 Best array pattern found by RGA for the 20-element array case with an improved null at the 3rd null; i.e., $\theta = 72.5°$ and $\theta = 107.5°$.

distribution, optimal inter-element spacing, initial depth and final null depth over the 3rd null position obtained by optimizing the cost function using RGA. In this case, the weightings of the array elements $I_1, I_2, \ldots I_M$ are normalized using max $(I_M) = 1$, and the inter-element spacings d are normalized by $\lambda/2$. Figs. 3–5 also depict the substantial reductions in the maximum peak of the SLL with non-uniform current excitation weights and optimal inter-element spacing, compared to the uniform current excitation weights and uniform inter-element spacing $(d = \lambda/2)$. Table 2A shows the SLL and FNBW of the optimized pattern for a null imposed at the 3rd null position.

Figs. 6–8 show the generation of nulls at the 3rd peak for 12, 16 and 20 element structures, respectively. For 12, 16, and 20 elements, the nulls have improved up to −123.5 dB, −83.17 dB, and −92.00 dB from the initial peak values of −19.56 dB, −20.10 dB, and −20.35 dB, respectively. Figs. 6–8 also depict the substantial reductions in the maximum peak

Table 2 Current excitation weights and initial and final null depths for a non-uniformly excited linear array with optimal inter-element spacing (d) for one null imposed in the 3rd null position.

No. of elements	$(I_1, I_2, \ldots I_M)$; d normalized with respect to $\lambda/2$	Initial depth (dB) (for $I_n = 1$ and $d = \lambda/2$)	Final depth (dB) (optimized I_n and d)
12	0.84511 0.6556 0.8444 0.71671 0.47139 0.40992; 1.1601	−51.90	−79.54
16	0.6013 0.5029 0.4866 0.4084 0.2438 0.1575 0.0173 0.0718; 1.1248	−50.60	−88.29
20	0.5478 0.7969 0.5051 0.5722 0.6221 0.6894 0.5206 0.4061 0.3769 0.1785; 1.2099	−77.20	−98.51

Table 2A SLL and FNBW for a non-uniformly excited linear array with optimal inter-element spacing (d) for one null imposed in the 3rd null position.

No. of elements	SLL final (dB)	FNBW final (degrees)
12	−16.76	19.10
16	−14.51	14.40
20	−15.50	11.52

of the SLL with the non-uniform current excitation weights and the optimal inter-element spacing compared to the uniform current excitation weights and a uniform inter-element spacing ($d = \lambda/2$). For example, in the optimized pattern, the SLL is reduced by more than 3 dB from −13.06 dB to −16.96 dB for the 12 element array. For the 16 element array with the optimized pattern, the SLL is reduced by more than 4 dB from −13.14 dB to −17.46 dB. For the 20 element array with the optimized pattern, the SLL is reduced by more than 1 dB from −13.19 dB to −14.22 dB. The improved values are shown in Tables 3 and 3A.

Figs. 9–11 show the generation of nulls at the 2nd and 3rd peaks for 12, 16 and 20 element structures, respectively. For 12, 16, and 20 elements, the pair of nulls has improved up to (−62.97 dB, −85.10 dB), (−83.87 dB, −69.09 dB), and (−71 dB, −78.92 dB) from the initial peak values of

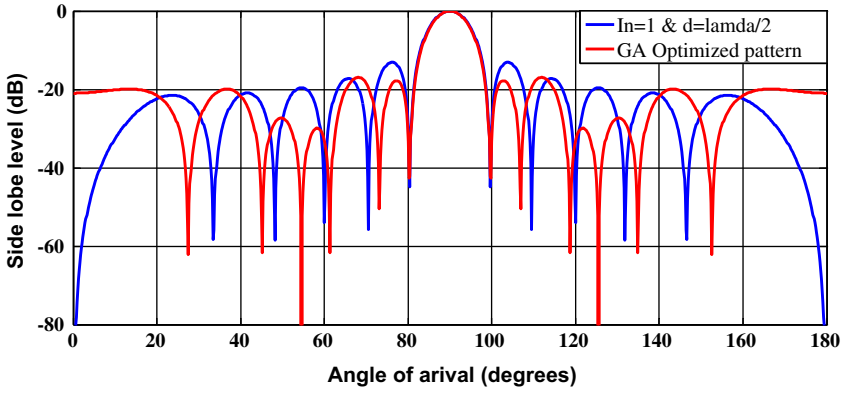

Figure 6 Best array pattern found by RGA for the 12-element array case with a null introduced at the 3rd peak; i.e., θ = 54.50° and θ = 125.50°.

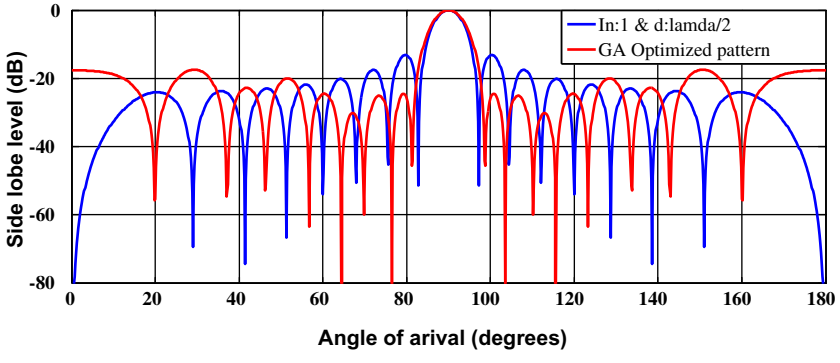

Figure 7 Best array pattern found by RGA for the 16-element array case with a null introduced at the 3rd peak; i.e., θ = 64.4° and θ = 115.6°.

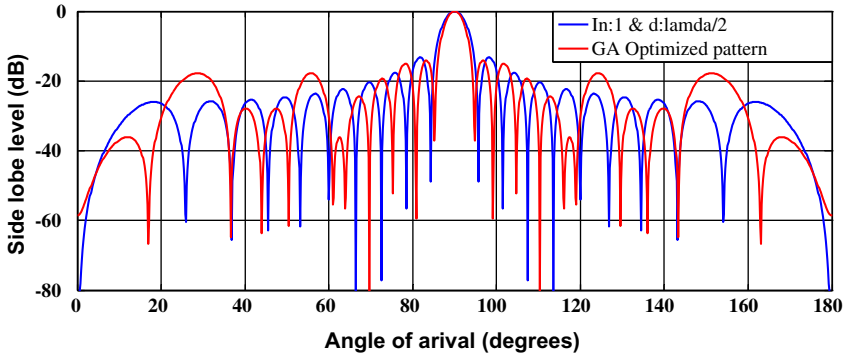

Figure 8 Best array pattern found by RGA for the 20-element array case with a null introduced at the 3rd peak; i.e., $\theta = 69.70°$ and $\theta = 110.30°$.

Table 3 Current excitation weights and initial and final null depths for a non-uniformly excited linear array with optimal inter-element spacing (d) for one null imposed in the 3rd peak position.

No. of elements	$(I_1, I_2, \ldots I_M)$; d normalized with respect to $\lambda/2$	Initial depth (dB) (for $I_n = 1$ and $d = \lambda/2$)	Final depth (dB) (optimized I_n and d)
12	0.60797 0.5196 0.40068 0.51144 0.3882 0.35568; 1.1273	−19.56	−123.5
16	0.5744 0.59995 0.45826 0.4777 0.39889 0.37541 0.14133 0.3515; 3.1903	−20.10	−89.17
20	0.8496 0.5783 0.8708 0.5555 0.5727 0.7696 0.6757 0.9098 0.3100 0.0361; 1.3892	−20.35	−92.00

Table 3A SLL and FNBW for a non-uniformly excited linear array with optimal inter-element spacing (d) for one null imposed in the 3rd peak position.

No. of elements	SLL final (dB)	FNBW final (degrees)
12	−16.96	19.08
16	−17.46	17.10
20	−14.22	10.00

(−17.22 dB, −19.56 dB), (−17.49 dB, −20.10 dB), and (−17.61 dB, −20.40 dB), respectively. Figs. 9–11 also depict the substantial reductions in the maximum peak of the SLL with the non-uniform current excitation weights and optimal inter-element spacing compared to the uniform current excitation weights and uniform inter-element spacing ($d = \lambda/2$). For example, the SLL is reduced by more than 3 dB from −13.06 dB to −16.17 dB for the 12 element array. For the 16 element array, the SLL is reduced by more than 6 dB from −13.14 dB to −20.00 dB. For the 20 element array, the SLL is reduced by more than 2 dB from −13.19 dB to −15.85 dB. The improved values are shown in Tables 4 and 4A.

Figs. 12–14 show the generation of nulls at the 2nd and 3rd nulls for 12, 16 and 20 element structures, respectively. For 12, 16, 20 elements, the pair of nulls has improved up to

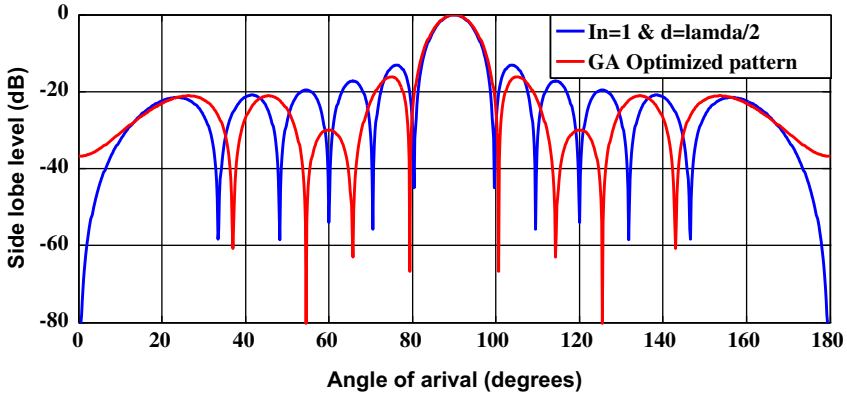

Figure 9 Best array pattern found by RGA for the 12-element array case with nulls introduced at the 2nd ($\theta = 65.7°, 114.3°$) and 3rd ($\theta = 54.50°, 125.50°$) peaks.

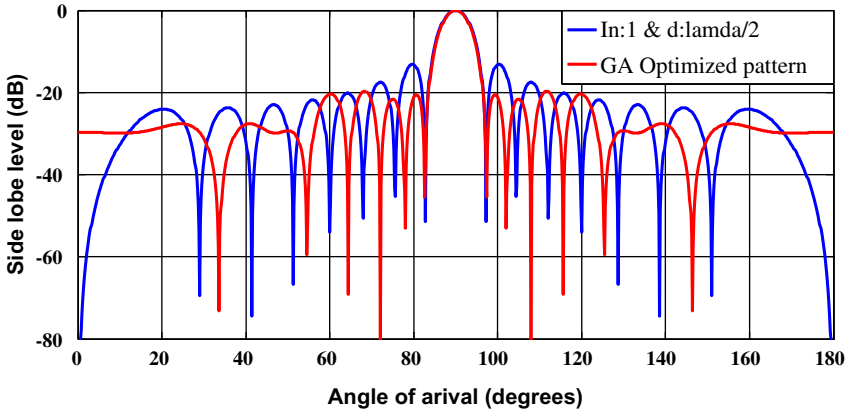

Figure 10 Best array pattern found by RGA for the 16-element array case with nulls introduced at the 2nd ($\theta = 72°, 108°$) and 3rd ($\theta = 64.4°, 115.6°$) peaks.

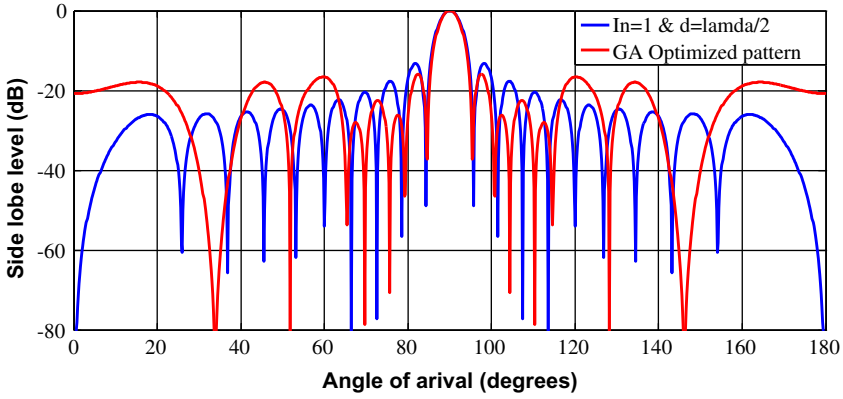

Figure 11 Best array pattern found by RGA for the 20-element array case with nulls introduced at the 2nd ($\theta = 75.6°, 104.4°$) and 3rd ($\theta = 69.7°, 110.3°$) peaks.

Table 4 Current excitation weights, initial peak depth and final null depth for a non-uniformly excited linear array with optimal inter-element spacing (d) for nulls imposed in the 2nd and 3rd peak positions.

No. of elements	$(I_1, I_2, \ldots I_M)$; d normalized with respect to $\lambda/2$	Initial depth (dB) (for $I_n = 1$ and $d = \lambda/2$) (2nd; 3rd)	Final depth (dB) (optimized I_n and d) (2nd; 3rd)
12	0.6876 0.7969 0.7023 0.67534 0.2092 0.1201; 1.2525	−17.22; −19.56	−62.97; −85.10
16	0.6049 0.5893 0.5405 0.5850 0.3186 0.3795 0.4347 0.2377; 1.2011	−17.49; −20.10	−83.87; −69.09
20	0.6163 0.5076 0.7290 0.4194 0.7148 0.2845 0.8719 0.3889 0.2575 0.5260; 1.0442	−17.61; −20.40	−71.00; −78.92

Table 4A SLL and FNBW for a non-uniformly excited linear array with optimal inter-element spacing (d) for nulls imposed at the 2nd and 3rd peak positions.

No. of elements	SLL final (dB)	FNBW final (degrees)
12	−16.17	21.22
16	−20.00	14.40
20	−15.85	11.52

(−82.75 dB, −94.66 dB), (−122.30 dB, −123.00 dB), and (−68.60 dB, −86.36 dB) from initial values of (−55.83 dB, −53.93 dB), (−45.35 dB, -50.60 dB), and (−56.62 dB, −77.2 dB), respectively. Figs. 12–14 also depict the substantial reductions in the maximum peak of the SLL with the non-uniform current excitation weights and optimal inter-element spacing compared to the uniform current excitation weights and uniform inter-element spacing ($d = \lambda/2$). For example, the SLL is reduced by more than 7 dB from −13.06 dB to −20.53 dB for the 12 element array. For the 16 element array,

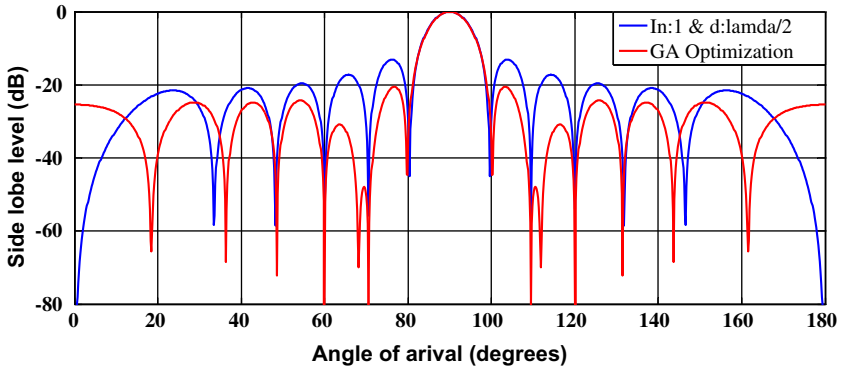

Figure 12 Best array pattern found by RGA for the 12-element array case with improved nulls at the 2nd ($\theta = 70.6°, 109.4°$) and 3rd ($\theta = 60°, 120°$) nulls.

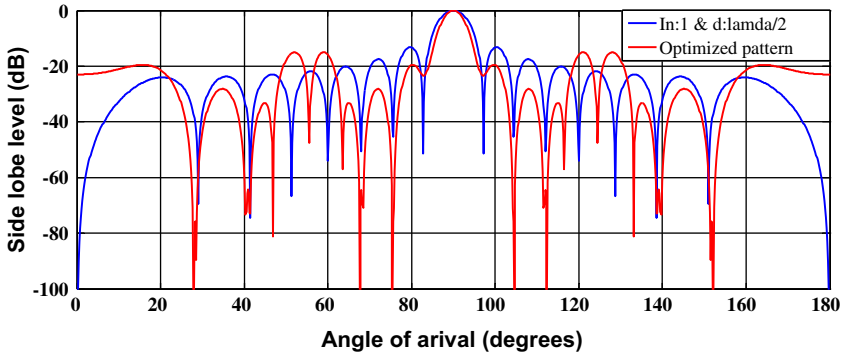

Figure 13 Best array pattern found by RGA for the 16-element array case with improved nulls at the 2nd ($\theta = 75.6°, 104.4°$) and 3rd ($\theta = 68°, 112°$) nulls.

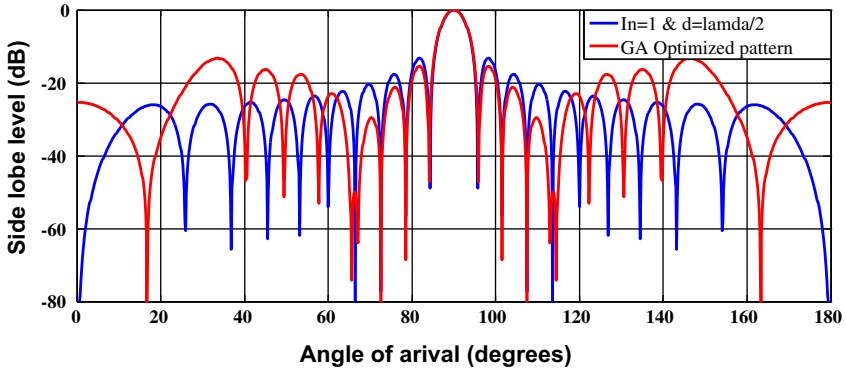

Figure 14 Best array pattern found by RGA for the 20-element array case with improved nulls at the 2nd ($\theta = 78.5°, 101.5°$) and 3rd ($\theta = 72.5°, 107.5°$) nulls.

Table 5 Current excitation weights and initial and final null depths for a non-uniformly excited linear array with optimal inter-element spacing (d) for nulls imposed in the 2nd and 3rd null positions.

No. of elements	$(I_1, I_2, \ldots I_M)$; d normalized with respect to $\lambda/2$	Initial depth (dB) (for $I_n = 1$ and $d = \lambda/2$) (2nd; 3rd)	Final depth (dB) (optimized I_n and d) (2nd; 3rd)
12	0.5974 0.5762 0.5642 0.4591 0.2516 0.2240; 1.2422	−55.83; −53.93	−82.75; −94.66
16	0.6198 0.5511 0.3251 0.4087 0.1548 0.2899 0.0937 0.1639; 1.7686	−45.35; −50.60	−122.30; −123.00
20	0.6163 0.5076 0.7290 0.4194 0.7148 0.2845 0.8719 0.3889 0.2575 0.5260; 1.0442	−56.62; −77.20	−68.60; −86.36

Table 5A SLL and FNBW for a non-uniformly excited linear array with optimal inter-element spacing (d) for nulls imposed at the 2nd and 3rd null positions.

No. of elements	SLL final (dB)	FNBW final (degrees)
12	−20.53	19.88
16	−15.05	14.40
20	−13.27	11.62

the SLL is reduced by approximately 2 dB from −13.14 dB to −15.05 dB. For the 20 element array, the SLL is reduced by less than 1 dB from −13.19 dB to −13.27 dB. The improved values are shown in Tables 5 and 5A.

5. Conclusions

This paper describes the design of a non-uniformly excited symmetric linear antenna array with optimized non-uniform spacings between the elements using the optimization techniques of a RGA. The simulated results reveal that optimizing the excitation values of the elements with the optimal inter-element spacings of the array antennas can impose deeper nulls in the interference direction and reduce the SLL for a given number of array elements with respect to the corresponding uniformly excited linear array with an inter-element spacing of $\lambda/2$. For instance, an optimized 16 element linear array antenna imposes nulls with values of −83.87 dB and −69.09 dB at the second and third peaks, respectively, from initial peak values of −17.49 dB and −20.10 dB at second and third peaks, respectively. The SLL was also reduced by 6.84 dB. The paper makes three main contributions: (i) In almost all design configurations, the null depth improves by approximately −80 dB. (ii) The maximum SLL is also reduced in all cases. (iii) The FNBW of the initial and final radiation pattern remains approximately the same. It is worth noting that although the proposed algorithm is implemented to constrain the synthesis of a linear array with isotropic elements, it is not limited to this case. The proposed algorithm can easily be implemented in non-isotropic element antenna arrays with different geometries to design various array patterns.

References

Abdolee, R., Ali, M.T., Rahman, T.A., 2007. Decimal genetics algorithms for null steering and sidelobe cancellation in switch beam smart antenna system. Int. J. Comput. Sci. Secur. 1 (3), 19–26.

Anooj, P.K., 2012. Clinical decision support system: risk level prediction of heart disease using weighted fuzzy rules. J. King Saud Univ. Comput. Inf. Sci. 24, 27–40.

Ares-Pena, F.J., Rodriguez-Gonzalez, J.A., Villanueva-Lopez, E., Rengarajan, S.R., 1999. Genetic algorithms in the design and optimization of antenna array patterns. IEEE Trans. Antennas Propag. 47 (3), 506–510.

Ballanis, C.A., 1997. Antenna Theory Analysis and Design, second ed. John Willey and Son's Inc, New York.

El Cafsi, M.A., Ghayoula, R., Trabelsi, Gharsallah, H., 2011. Phased uniform linear antenna array synthesis using genetic algorithm. In: 11th Mediterranean Microwave Symposium (MMS 2011), Hammamet, Category number FP1146H-ART; Code 87531, 8–10 September.

Das, S., Bhattacharjee, S., Mandal, D., Bhattacharjee, A.K., 2010. Optimal sidelobe reduction of symmetric linear antenna array using genetic algorithm. In: IEEE INDICON 2010, Dec 17–19, Kolkata, India.

De, I., Sil, J., 2012. Entropy based fuzzy classification of images on quality assessment. J. King Saud Univ. Comput. Inf. Sci. 24, 165–173.

Elliott, R.S., 2003. Antenna Theory and Design, revised ed. John Wiley, New Jersey.

Fahmy, A.A., 2012. Using the bees algorithm to select the optimal speed parameters for wind turbine generators. J. King Saud Univ. Comput. Inf. Sci. 24, 17–26.

Guney, K., Akdagli, A., 2001. Tabu search algorithm for the optimal pattern synthesis of linear antenna arrays with broad nulls. J. Marm. Pure Appl. Sci. 17 (2), 61–70.

Haupt, R.L., 1995. An introduction to genetic algorithm for electromagnetic. IEEE Antennas Propag. Mag. 37 (2), 7–15.

Haupt, R.L., 1997. Phase-only adaptive nulling with a genetic algorithm. IEEE Trans. Antennas Propag. 45 (6), 1009–1015.

Haupt, R.L., Werner, D.H., 2007. Genetic Algorithms in Electromagnetics. IEEE Press Wiley-Interscience.

Holland, J.H., 1975. Adaptation in Natural and Artificial Systems. University Michigan Press, Ann Arbor.

Mandal, D., Ghoshal, S.P., Bhattacharjee, A.K., 2009. Determination of the optimal design of three-ring concentric circular antenna array using evolutionary optimization techniques. Int. J. Recent Trends Eng. 2 (5), 110–115.

Mandal, D., Yallaparagada, N.T., Ghoshal, S.P., Bhattacharjee, A.K., 2010. Wide null control of linear antenna arrays using particle swarm optimization. In: IEEE INDICON 2010, Dec 17–19, Kolkata, India.

Mandal, S., Ghoshal, S.P., Kar, R., Mandal, D., 2012. Design of optimal linear phase fir high pass filter using craziness based particle swarm optimization technique. J. King Saud Univ. Comput. Inf. Sci. 24, 83–92.

Mondal, D., Chandra, A., Ghoshal, S.P., Bhattacharjee, A.K., 2010. Side lobe reduction of a concentric circular antenna array using genetic algorithm. Serb. J. Electr. Eng. 7 (2), 141–148.

Mukherjee, S., Kar, S., 2012. Application of fuzzy mathematics and grey systems in education. J. King Saud Univ. Comput. Inf. Sci. 24, 157–163.

Recioui, A., Azrar, A., Bentarzi, H., Dehmas, M., Chalal, M., 2008. Synthesis of linear arrays with sidelobe level reduction constraint using genetic algorithms. Int. J. Microwave Opt. Technol. 3 (5), 524–530.

Son, S.H., Park, U.H., 2007. Sidelobe reduction of low-profile array antenna using a genetic algorithm. ETRI J. 29 (1), 95–98.

Steyskal, H., Shore, R.A., Haupt, R.L., 1986. Methods for null control and their effects on the radiation pattern. IEEE Trans. Antennas Propag. 34 (3), 404–409.

Yan, K.K., Lu, Y., 1997. Sidelobe reduction in array-pattern synthesis using genetic algorithm. IEEE Trans. Antennas Propag. 45, 1117–1122.

Yang, S., Gan, Y.B., Qing, A., 2002. Sideband suppression in time-modulated linear arrays by the differential evolution algorithm. IEEE Antennas Wirel. Propag. Lett. 1, 173–175.

Yang, S., Gan, Y.B., Qing, A., 2004. Antenna-array pattern nulling using a differential evolution algorithm. Int. J. RF Microwave Comput. Aided Eng. 14 (1), 57–63.